

Supporting Information

Ex Situ CdSe Quantum Dot Sensitized Solar Cells Employing Inorganic Ligand Exchange to Boost Efficiency

Feng Liu,^a Jun Zhu,^{*a} Junfeng Wei,^a Yi Li,^a Linhua Hu,^a Yang Huang,^a Oshima Takuya,^b Qing Shen,^{*b,c} Taro Toyoda,^{b,c} Bing Zhang,^d Jianxi Yao^d and Songyuan Dai^{*a,d}

^aKey Laboratory of Novel Thin Film Solar Cells, Institute of Plasma Physics, Chinese Academy of Sciences, P.O. Box 1126, Hefei, Anhui 230031, P. R. China

^bDepartment of Engineering Science, Faculty of Informatics and Engineering, The University of Electro-Communications, 1-5-1 Chofugaoka, Chofu, Tokyo 182-8585, Japan

^cCREST, Japan Science and Technology Agency (JST), 4-1-8 Honcho Kawaguchi, Saitama 332-0012, Japan

^dSchool of Renewable Energy, North China Electric Power University, Beijing, 102206, P. R. China

1. Optical Property and TEM image of Colloidal CdSe QDs

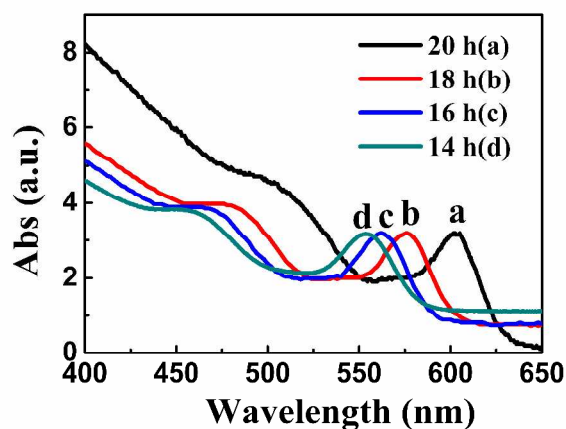


Figure S1. UV-vis absorption spectra of the organic ligands-capped CdSe QDs in chloroform solvent. Different first exciton absorption peaks were obtained when varying QDs' growth time: 14 h, 16 h, 18 h, 20 h. This figure also confirms the important property of size-dependent tunable band gap of the pre-synthesized QDs.

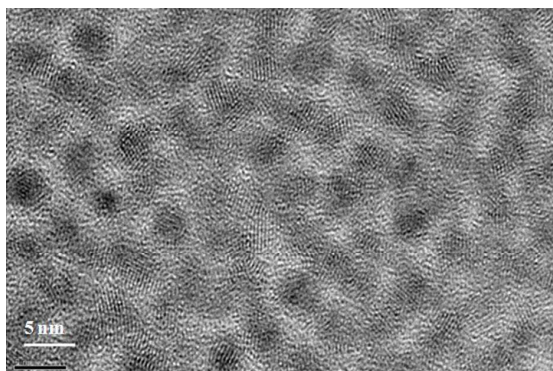


Figure S2. Transmission electron microscopy (TEM) micrograph of the colloidal CdSe QDs.

UV-vis absorption spectra (Figure S1) reveal that the first exciton peak of CdSe QDs was redshifted as the reaction time prolonged, indicating the growth of QDs over time. The size of the CdSe nanocrystal can be calculated from Peng's calibration data equation.¹ The size distribution of CdSe QDs was measured from the half-widths at half-maxima of the exciton absorption peaks in UV-vis absorption spectra. The width of the excitonic peak is indicative of a $\pm 1.25\%$ distribution of particle sizes (estimated from the comparison of ref. 2²). The transmission electron microscopy (TEM) image (Figure S2) of the TOP-capped CdSe nanocrystals reveals that the resulting nanocrystals have a narrow size distribution, which is well consistent with the result of UV-vis absorption spectrum. The spectra of the ex situ CdSe are quite different from that in the in situ route for the latter always exhibits a broad size dispersion.

2. QDs' Adsorption to Mesoporous TiO₂ Films

The sensitization of photoanode was realized by immersing the TiO₂ films into the organic ligands-capped CdSe QDs chloroform solution. QDs' adsorption to mesoporous TiO₂ films can be divided into two processes: Langmuir isotherm-like dominated submonolayer adsorption and QDs aggregation processes.³ The total increase in QD concentration adsorbed on TiO₂ films can be given by eqs 1.

$$\frac{d[p]_{\text{Total}}}{dt} = \frac{d[p]_{\text{Lang}}}{dt} + \frac{d[p]_{\text{ag}}}{dt} \quad (1)$$

$[p]_{\text{Total}}$, $[p]_{\text{Lang}}$, $[p]_{\text{ag}}$ represent the total concentration of CdSe QDs adsorbed on TiO₂ films, Langmuir-type submonolayer adsorption concentration and aggregation contributed concentration, respectively. To optimize the performance of the photoanode, QDs' deposition time should be carefully chosen. Adsorption time influences the total loading of QDs into mesoporous TiO₂, which is supposed to be better if more QDs loaded onto electron acceptors in consideration of light harvesting. However, the adsorption time should come to a compromise with the loading amount because of the inevitable QD particles' agglomeration on TiO₂ surface which would deteriorate the charge transportation within nanoporous TiO₂ network and electrolyte conductors' penetration for hole extracting.

3. X-ray Diffraction Patterns

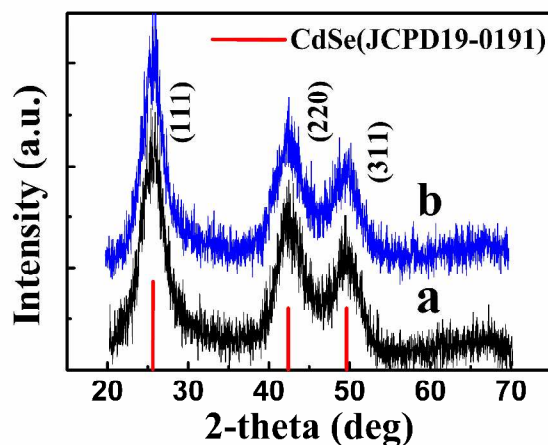


Figure S3. X-ray diffraction patterns of (a) CdSe, (b) CdSe with S²⁻ solution treated. Sample preparation for XRD measurement was done by dropping CdSe QDs suspension onto a clean glass and allowing it to dry at room temperature. S²⁻ treatment was performed by immersing the CdSe QDs-covered glass into Na₂S solution for 46 h and finally rinsed with pure water and methanol.

4. FT-IR

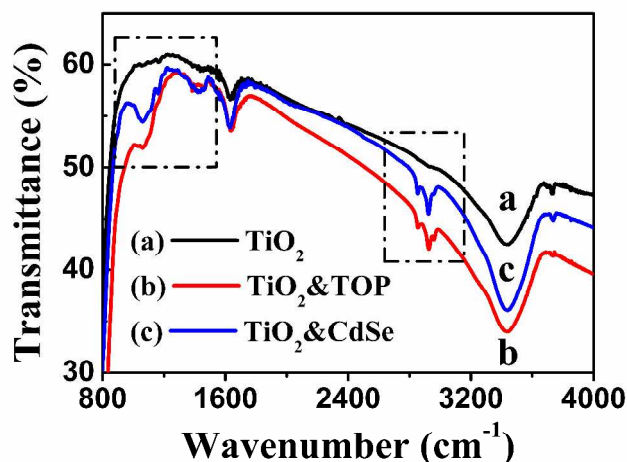


Figure S4. FT-IR spectra. The broad absorption peak at 1000 cm^{-1} - 1145 cm^{-1} appears in sample b and c, as well as the C-H signal peak at 2853 cm^{-1} and 2923 cm^{-1} , both reveal the fact that these peaks are assigned to TOP signal and CdSe QDs are initially TOP ligands capped. Sample b and c were prepared by immersing the TiO_2 films into TOP and CdSe solution respectively for 24 h and subsequently rinsed with water/methanol and finally dried in N_2 condition.

5. Ruling out the Influence that S^{2-} Treatment Bring on Changing the Property of TiO_2 Nanoparticles

We first study the adsorption kinetics of sulfur ions when contact with TiO_2 nanoparticles. A typical UV-vis absorption test of CdS QDs which deposited onto TiO_2 mesoporous films by SILAR method was carried out by differing the sequence of dipping in cadmium and sulfur precursor solution. Sample a: $\text{TiO}_2 + \text{Cd}^{2+}$ (first) + S^{2-} , sample b: $\text{TiO}_2 + \text{S}^{2-}$ (first) + Cd^{2+} , both were washed thoroughly with the corresponding solvent after each dipping process and the SILAR process was performed for only one cycle, 10 min for each dipping. Figure S5 shows a clear difference in absorption spectra between sample a and b. We can see an obvious absorption enhancement in 370 nm-440 nm wavelength range compared with the blank TiO_2 reference, indicating the formation of CdS layer in sample a, whose TiO_2 film was first dipped into cadmium precursor solution. It's believed that Cd^{2+} would attach to the TiO_2 nanoparticle, reacting with S^{2-} that comes after. However, the absorption spectrum exhibits no change when we first put the TiO_2 film into the sulfur precursor solution, confirming that the CdS reaction didn't occur within the network of TiO_2 . Therefore, it's reasonable to assume that the TiO_2 nanoparticle has no any affinity for sulfur ion, thus also ruling out the probability that the detected S signal in EDS spectra come from the TiO_2 film. We further to observe the influence that immersing into Na_2S solution would bring on changing the chemical property of TiO_2 nanoparticles by evaluating the binding energy of Ti 2p in XPS spectra. As seen in Figure S6, the binding energy of Ti $2p_{3/2}$ and Ti $2p_{1/2}$ rarely changed after immersing into the S^{2-} solution. Herein, we can draw conclusion that immersing into the S^{2-} solution do not change the property of TiO_2 , excluding its role in changing the performance of the photoanodes during S^{2-} treatment.

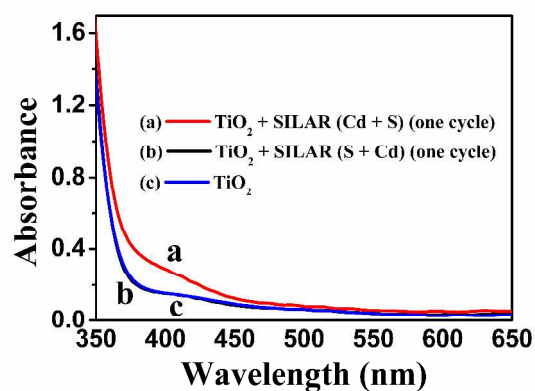


Figure S5. UV-vis absorption spectra. (a) TiO_2 + Cd (first) + S, (b) TiO_2 + S (first) + Cd and (c) blank TiO_2 film. Thickness of the TiO_2 films used here was about 3 μm .

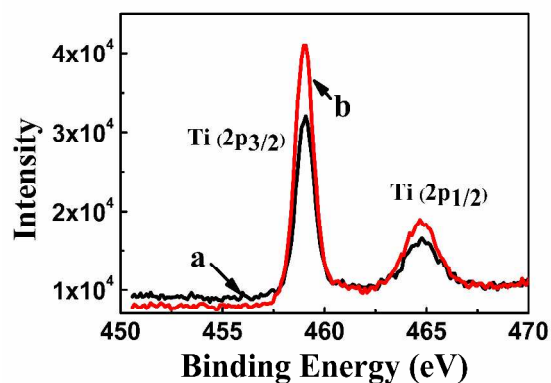


Figure S6. XPS spectra of Ti $2p_{3/2}$ and Ti $2p_{1/2}$ in TiO_2 film. (a) untreated sample (b) S^{2-} treated sample.

6.

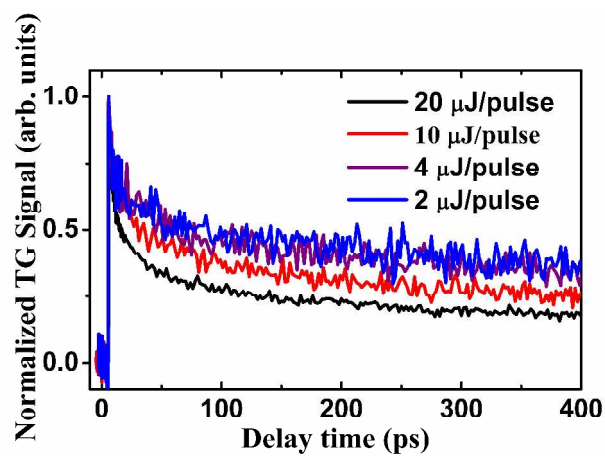


Figure S7. Dependence of TG responses of CdSe adsorbed TiO_2 film with TOP capping on the pump light intensity.

7. SILAR Prepared CdSe QDs Sensitized Photoanodes and Its S^{2-} Treatment

CdSe QDs sensitized TiO₂ photoanodes prepared by SILAR method were mainly according to Lee et al.'s previous report⁴ with slight modification. In a N₂-filled glove box, cadmium precursor was prepared by dissolving 0.185 g Cd(NO₃)₂·4H₂O in 20 ml ethanol and Se²⁻ was prepared by reducing 0.1 g SeO₂ with 0.068 g NaBH₄ in 30 ml ethanol. The TiO₂-modified electrode was dipped into the above precursors for QD's deposition. The immersion cycle was repeated 5 times and 6 min for each deposition.

S²⁻ treatment for SILAR-prepared photoanodes was carried out as described in the case of the as-synthesized photoanodes.

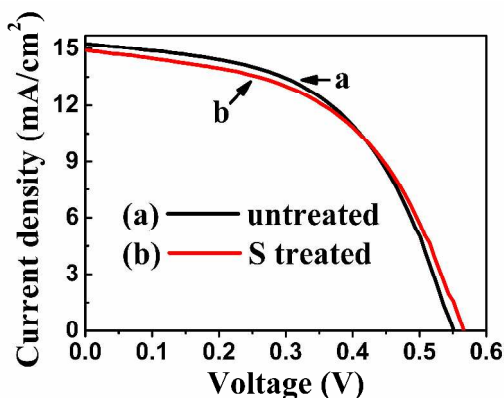


Figure S8. *J-V* characteristics of the CdSe QDSSCs prepared by SILAR.

Table S1. Photovoltaic parameters of QDSSCs prepared by SILAR under different conditions.

Device	V_{oc} (V)	J_{sc} (mA/cm ²)	FF (%)	η (%)
Untreated	0.54	15.34	52.03	4.31
S ²⁻ treated	0.56	15.00	51.20	4.30

REFERENCES

- (1) Yu, W. W.; Qu, L. H.; Guo, W. Z.; Peng, X. G. Experimental determination of the extinction coefficient of CdTe, CdSe, and CdS nanocrystals. *Chem. Mater.* **2003**, *15*, 2854-2860.
- (2) Qu, L. H.; Peng, X. G. Control of photoluminescence properties of CdSe nanocrystals in growth. *J. Am. Chem. Soc.* **2002**, *124*, 2049-2055.
- (3) Pernik, D. R.; Tvrđy, K.; Radich, J. G.; Kamat, P. V. Tracking the Adsorption and Electron Injection Rates of CdSe Quantum Dots on TiO₂: Linked versus Direct Attachment. *J. Phys. Chem. C* **2011**, *115*, 13511-13519.
- (4) Lee, H.; Wang, M. K.; Chen, P.; Gamelin, D. R.; Zakeeruddin, S. M.; Gratzel, M.; Nazeeruddin, M. K. Efficient CdSe Quantum Dot-Sensitized Solar Cells Prepared by an Improved Successive Ionic Layer Adsorption and Reaction Process. *Nano Lett.* **2009**, *9*, 4221-4227.